Recent developments in the NPDD model

Michael R. Gleeson[1], Jinxin Guo[2], and John T. Sheridan[2]

[1]Department of Computer Science, National University of Ireland Maynooth,
Maynooth, Co. Kildare, Republic of Ireland.

[2]UCD School of Electrical, Electronic and Communications Engineering,
College of Engineering, Mathematical and Physical Sciences,
Communications and Optoelectronic Research Centre,
SFI Strategic Research Centre in Solar Energy Conversion,
University College Dublin, Belfield, Dublin 4, Republic of Ireland.

ABSTRACT

An understanding of the photochemical and photo-physical processes, which occur during photo-polymerization, is of extreme importance when attempting to improve a photopolymer material's performance for a given application. Recent work carried out on the modeling of photopolymers during- and post-exposure, has led to the development of a tool, which can be used to predict the behavior of a number of photopolymers subject to a range of physical conditions. In this paper, we explore the most recent developments made to the Non-local Photo-polymerization Driven Diffusion model, and illustrate some of the useful trends, which the model predicts and then analyze their implications on photopolymer improvement.

Keywords: Holography, holographic recording material, photopolymer, inhibition.
Contact Author: mgleeson@cs.nuim.ie and john.sheridan@ucd.ie

1. INTRODUCTION

Extensive research and development of photopolymer materials and their photochemical kinetics [1-10] has been carried out in both academia and industry due to the growing interests in applications involving photopolymers [12-19]. To maximise the potential of these materials, the provision of a physically comprehensive theoretical model of the effects occurring during and post- photo-polymerization is becoming ever more important. Such a model will enable potential trends in a material's performance to be recognized and optimised, [20-30]. An example of this is the two part paper published by Guo *et al*. [31,32] whereby chain transfer agents were added to reduce the effects of non-local polymer chain growth and hence improve the high density resolution of the photopolymer under examination.

A recent publication by the authors [33] has presented a number of simulations of ratios of various key material components which offer possible methods to further improve photopolymer materials. This model's versatility has also been shown through its application to a number of other photopolymers, [34,35] including a material developed by Bayer MaterialScience (BMS), Germany. In this paper we extend the Non-local Photo-polymerization Driven Diffusion (NPDD) model used in the analysis provided in Ref. [33], to generate a more physically accurate representation of the processes occurring during photo-polymerisation. These extensions include;

(i) time varying kinetic rates of reactions as a result of increased material viscosity (reduction in free volume),
(ii) temporal and spatial variations in monomer and polymer diffusion due to increased material viscosity,
(iii) full multicomponent analysis, inclusive of free space hole generation,
(iv) independent monomer and crosslinker reactions and diffusion effects,
(v) inter-diffusion effects between monomers and free space holes.

It must also be clearly noted at this point, that the model includes; (a) non-steady state kinetics, (b) spatial and temporal non-local polymer chain growth, (c) time varying photon absorption, (d) temporal and spatial primary radical generation, (e) the effects of both primary and bimolecular termination, and (f) polymerisation inhibitory effects.

This paper is structured as follows. In Section 2 we examine the photochemical processes involved during holographic grating formation, implementing the various extensions to the model which are listed above. The governing set of truncated first-order coupled differential equations for this more physically accurate improved model can then be generated. Then in Section 3 by applying suitable initial conditions, the first-order coupled differential equations are solved numerically and simulations highlighting the predictions of the extended model are made.

2. NPDD Model

2.1 Photo-kinetics

The photochemical processes, which are present during photo-polymerization, are complex; however an understanding of these processes is of utmost importance in the production of a material optimisation tool. In a recent review, [30] many of the assumptions made in developing photochemical models of free radical photo-polymerisation were discussed and a number of physical effects which were not included in the current models were listed indicating a lack of physicality under certain exposure conditions. Following the appearance of this review, a series of papers were published, [9-11] which addressed many of these issues and provided a model containing a consistent set of chemical reaction equations to take into account many of these neglected effects. In this paper, we further develop and extend this NPDD model to include a number of the outstanding processes which were not included in this series of papers [9-11]. The resulting reaction mechanisms which constitute this model are listed as follows in Eqs (1-4):

I. Initiation,

$$D + h\upsilon \xrightarrow{ka} D^{*}, \tag{1a}$$

$$D^{*} + Z \xrightarrow{kz,D} Leuco\ Dye, \tag{1b}$$

$$D^{*} \xrightarrow{kr} D, \tag{1c}$$

$$D^{*} + CI \xrightarrow{kd} R^{\bullet} + H^{+} + D^{\bullet -} \longrightarrow R^{\bullet} + HD^{\bullet}, \tag{1d}$$

$$CI + HD^{\bullet} \xrightarrow{kb} H_2D + CI_{\text{int}}, \tag{1e}$$

$$R^{\bullet} + M_A \xrightarrow{k_{iA}} M^{\bullet}_{1,A} + HoleA, \tag{1f}$$

$$R^{\bullet} + M_B \xrightarrow{k_{iB}} M^{\bullet}_{1,B} + HoleB. \tag{1g}$$

where D represents the concentration of photosensitiser (dye), $h\nu$ represents the photon energy incident on the material, D^{*} is the excited state of the dye, CI is the co-initiator, $R^{\bullet}$ represents the primary radical concentration, Z is the inhibitor, $HD^{\bullet}$ represents a radicalised dye, which has abstracted a hydrogen from the co-initiator, and H_2D is the di-hydro transparent form of the dye. CI_{int} is an intermediate form of the co-initiator, which is no longer available for reaction. k_r (s^{-1}) is the rate of recovery or regeneration of photo-absorber, k_d ($cm^3mol^{-1}s^{-1}$) is the rate of dissociation of the initiator, k_b ($cm^3mol^{-1}s^{-1}$) is the rate associated with photo-bleaching of the dye and $k_{z,D}$ ($cm^3mol^{-1}s^{-1}$) is the inhibition rate constant associated with the reaction with excited dye molecules. The rate of production of the excited state photosensitiser, appearing in Eq (1a) can be represented by $k_a = \phi \varepsilon d I_0^{'}$ (s^{-1}), where ϕ (mol/Einstein) is the quantum efficiency of the reaction, ε (cm^2/mol) is the molar absorptivity, and d (cm) is the material layer thickness [11]. If the photosensitiser's initial concentration, molar absorptivity, quantum efficiency, and layer thickness are known, the rate

of generation of excited state photosensitiser, D^*, can be determined for a given exposure intensity. For a full examination of the steps involved in the Initiation mechanisms, see Ref [11].

M_A and M_B represent the monomer and crosslinker concentrations respectively, $M^{\bullet}_{1,A}$ and $M^{\bullet}_{1,B}$ represent growing macroradicals (or chain initiator species) of length $n = 1$. *HoleA* and *HoleB* denote the free volume vacuoles created by breaking the carbon double bonds when the monomer and crosslinker are polymerised. The rates of initiation k_{iA} and k_{iB} ($cm^3mol^{-1}s^{-1}$) incorporate the variation in the material's fractional free volume as a result of the photo-polymerisation of the monomers and will be discussed in more detail later in the paper.

II. Propagation,

$$M^{\bullet}_n + M_A \xrightarrow{k_{pA}} M^{\bullet}_{n+1} + HoleA, \tag{2a}$$

$$M^{\bullet}_n + M_B \xrightarrow{k_{pB}} M^{\bullet}_{n+1} + HoleB. \tag{2b}$$

III. Termination,

$$M^{\bullet}_n + M^{\bullet}_m \xrightarrow{k_{tc}} M_{n+m} = Dead\ Polymer, \tag{3a}$$

$$M^{\bullet}_n + M^{\bullet}_m \xrightarrow{k_{td}} M_n + M_m = Dead\ Polymer, \tag{3b}$$

$$M^{\bullet}_n + R^{\bullet} \xrightarrow{k_{tp}} M_nR = Dead\ Polymer. \tag{3c}$$

In Eqs (2) and (3), $M^{\bullet}_n$, $M^{\bullet}_m$ and $M^{\bullet}_{n+1}$ represent growing macroradical chains of length *n*, *m* and *n*+1. In the NPDD model discussed later, these growing macroadical chains (polymer) represent the number of carbon double bonds which are broken by polymerisation, but say nothing about the number of repeat monomeric units in the polymer chains. M_n, M_m, M_{n+m}, M_nR denote terminated polymer species with no active propagating tip, i.e. *Dead Polymer*. k_{tc} and k_{td} ($cm^3mol^{-1}s^{-1}$) are the rate constants of termination by combination and termination by disproportionation respectively, which for this analysis will be combined into one kinetic constant k_t. We note that the polymer chains produced by the polymerisation of monomer, M_A, and the polymer chains produced by the polymerisation of crosslinker, M_B, are assumed to be of the same species with the same physical attributes, i.e. refractive index.

The kinetic rate constants, k_{iA}, k_{iB}, k_{pA}, k_{pB} and k_t, in Eqs (1), (2) and (3), are in general dependent on the viscosity of a photopolymer material. As polymerization proceeds, the resulting increase in viscosity of the material, (due to densification and cross-linking), can cause a significant reduction in the mobility of large molecules, (growing polymer chains. When the diffusional limitations become large enough to restrict the diffusion of growing polymer chains, they can no longer diffuse into close enough proximity to react with other macroradicals, and as a result the termination rate, k_t, decreases. This decrease in termination leads to a build-up in macroradical concentration, which subsequently causes a sudden increase in the rate of polymerization, which is known as *autoacceleration*, (*gel* or *Trommsdorff* effect), [35]. Once termination drops below a critical level, a different mechanism will become dominant, this mechanism is known as *reaction-diffusion*.

Reaction-diffusion-controlled termination arises when termination is controlled by the ability of monomer, M_A and crosslinker, M_B molecules and to diffuse to the restricted active macroradical tips. It occurs when the termination of a macroradical is faster and more likely to take place, due to the *continued growth* of a propagating chain (until it encounters another macroradical for bimolecular termination), than it is likely to *diffuse to* and thus 'locate' another macroradical chain for termination by bimolecular termination. Since the controlling step in this termination mechanism relies on macroradical chain growth, (propagation through available monomer), the termination kinetic

constant becomes dependent on the propagation kinetic constant, as indicated in Eq (4), (an amended version of the analysis provided by Goodner *et al*.) [3,4],

$$k_t = \frac{k_{t0}}{1+\left\{\frac{R_{DA}k_{pA}M_A}{k_{t0}}+\frac{R_{DB}k_{pB}M_B}{k_{t0}}+\exp\left[-A_t\left(\frac{1}{f^v}-\frac{1}{f_{ct}^v}\right)\right]\right\}^{-1}}. \tag{4}$$

where k_{t0} is the initial termination kinetic constant in the absence of diffusional limitations, R_{DA} and R_{DB} are the reaction diffusion parameters defined as the termination kinetic constant in the reaction-diffusion region divided by the product of the initial propagation kinetic constant and the instantaneous un-reacted monomer, M_A, or crosslinker, M_B, concentrations.

f^v is the fractional free volume of the system, [3,4], and f_{ct}^v is the critical fractional free volume at which termination becomes diffusionally controlled and A_t is a parameter which governs the rate at which the termination kinetic constant decreases in this diffusion controlled region. As the monomer and crosslinker molecules are converted to polymer, there is a resulting increase in the material's viscosity. This increase in viscosity results in a reduction in the amount of free volume in the photopolymer material and hence leads to diffusional limitations. The variation in fractional free volume can be described using the equation,

$$f^v = f_{emp} + \sum \phi_i \alpha_i \left(T - T_{gi}\right), \tag{5}$$

where f_{emp} is an assumed empirical free volume of each of the components at their glass transition temperatures. ϕ_i is the volume fraction of each constituent of the material, α_i (L/C) is the expansion coefficient of each component, T_{gi} (C) are the glass transition temperatures of the components and T (C) is the local temperature. All of these parameters can be readily measured or determined.

Returning to the processes occurring during exposure, as the viscosity effects begin to increase further, the mobility of un-reacted monomer molecules, M_A, and crosslinker molecules, M_B, become even more limited. Under these conditions, monomer and crosslinker can no longer easily diffuse to the reactive sites and as a result the propagation rates, k_{pA} and k_{pB}, and consequently the rate of polymerisation, decreases. This effect is known as *autodeceleration*, [3,4,35]. Again following the work presented by Goodner *et al*., [3,4], on the effects of viscosity changes on the propagation, we write that,

$$k_{pA} = \frac{k_{pA0}}{1+\exp\left[A_{pA}\left(\frac{1}{f^v}-\frac{1}{f_{cpA}^v}\right)\right]}, \tag{6a}$$

$$k_{pB} = \frac{k_{pB0}}{1+\exp\left[A_{pB}\left(\frac{1}{f^v}-\frac{1}{f_{cpB}^v}\right)\right]}, \tag{6b}$$

where k_{pA0} and k_{pB0} are the initial propagation kinetic constants of monomer and crosslinker in the absence of diffusional limitations, f_{cpA}^v and f_{cpB}^v are the critical fractional free volumes of monomer and crosslinker at which

propagation becomes diffusionally controlled and A_{pA}, and A_{pB} are the parameters which governs the rate at which the propagation kinetic constants decreases in this diffusion controlled region.

Similarly, the diffusion controlled kinetic constants for the rate of initiation, k_{iA} and k_{iB}, will be of the same form as the propagation rates, giving the expressions,

$$k_{iA} = \frac{k_{iA0}}{1+\exp\left[A_{iA}\left(\frac{1}{f^{v}} - \frac{1}{f_{ciA}^{v}}\right)\right]}, \tag{7a}$$

$$k_{iB} = \frac{k_{iB0}}{1+\exp\left[A_{iB}\left(\frac{1}{f^{v}} - \frac{1}{f_{ciB}^{v}}\right)\right]}, \tag{7b}$$

where, k_{iA0}, k_{iB0} are the initial initiation kinetic constants of monomer and crosslinker in the absence of diffusional limitations, A_{iA} and A_{iB} are the rates at which the initiation kinetic constant decreases in the diffusion controlled region and f_{ciA}^{v} and f_{ciB}^{v} are the critical fractional free volumes of monomer and crosslinker at which initiation becomes diffusionally controlled.

It must be noted at this point that as the monomer and crosslinker are different species, with different behaviours, their kinetic constants will also differ. Thus the onset of diffusional limitations and the rate at which the kinetic constants decrease in the diffusion controlled region will be different. Simulations presented later in the paper will highlight these effects.

IV. Inhibition,

$$D^{*} + Z \xrightarrow{k_{z,Dye^{*}}} LeucoDye + Z^{*}, \tag{8a}$$

$$R^{\bullet} + Z \xrightarrow{k_{z,R^{\bullet}}} \left(R + Z^{\bullet}\text{, and/or } RZ^{\bullet}\right) = Scavenged\ Radical, \tag{8b}$$

$$M_n^{\bullet} + Z \xrightarrow{k_{z,M^{\bullet}}} \left(M_n + Z^{\bullet}\text{, and/or } M_nZ^{\bullet}\right) = Dead\ Polymer. \tag{8c}$$

In Eq (8), Z denotes the inhibitor concentration, $M_nZ^{\bullet}$ represents polymer species which have no active propagating tip, i.e. *Dead Polymer* and Z^{*} is the concentration of singlet oxygen [11]. As before the term *Dead Polymer* signifies the cessation of the growth of a propagating macroradical of *n* monomer repeat units, [35], while the term *Scavenged Radical* signifies the removal of a primary radical, [11].

2.2 Coupled Differential Equations

When recording holographic gratings in photopolymers, a co-sinusoidal spatial distribution of irradiance is used, which can be represented as $I(x,t) = I_0'\left[1 + V\cos(Kx)\right]$, where V is the fringe visibility and $K = 2\pi/\Lambda$, where Λ is the grating period. The exposure intensity in (Einsteins/cm^{3}s) is $I_0' = \frac{T_{sf} B I_0}{d}\left(\frac{\lambda}{N_a hc}\right)$, where I_0 (mW/cm^2) is the incident intensity, λ (nm) is the wavelength of incident light, N_a (mol^{-1}) is Avogadro's constant, c (m/s) is the speed of light, and h (Js) is Plank's constant. $B = 1 - \exp(-\varepsilon D_0 d)$, is the absorptive fraction which determines a material

layer's initial absorptive capacity and is a function of the dye's initial concentration D_0 (mol/cm^3), T_{sf} a fraction associated with the light lost by Fresnel and scattering losses, and the material's molar absorptivity and layer thickness [11].

The spatial variation in irradiance sets up spatial concentration gradients of the constituents of the photopolymer through the photo-kinetic reactions presented in Section 2.1, yielding a set of first-order coupled differential equations which form the NPDD model. These equations are presented in the following subsections, through Eqs (9–15) and Eqs (22) and (24-27), with all parameters and notation as presented above unless otherwise specified. Note that all equations are coupled together, but have been grouped by relevance to make it easier for the reader to follow.

2.2.1 Absorptive Species

The first set of coupled differential equations deal with the absorptive species, which consists of the photosensitiser and the co-initiator with subsequent reactions and photo-products.

$$\frac{dD(x,t)}{dt} = -k_a D(x,t) + k_r D^*(x,t), \tag{9}$$

$$\frac{dD^*(x,t)}{dt} = k_a D(x,t) - k_r D^*(x,t) - k_d D^*(x,t) CI(x,t) - k_{z,D} D^*(x,t) Z(x,t), \tag{10}$$

$$\frac{dCI(x,t)}{dt} = -k_d D^*(x,t) CI(x,t) - k_b HD^\bullet(x,t) CI(x,t), \tag{11}$$

$$\frac{dHD^\bullet(x,t)}{dt} = k_d D^*(x,t) CI(x,t) - k_b HD^\bullet(x,t) CI(x,t), \tag{12}$$

2.2.2 Oxygen Inhibtion

As in the previous analysis, [9-11] it is assumed that the effect of inhibition during exposure is due solely to the initially dissolved oxygen present within the photopolymer layer. The non-uniform recording irradiance causes concentration gradients of oxygen as it is consumed in inhibitory reactions. This then results in the diffusion of oxygen from the dark non-illuminated regions to the bright illuminated regions. As oxygen molecules are small compared to the other material components which constitute the photopolymer layer, it can be assumed that the oxygen is relatively free to diffuse rapidly, resulting in a one-dimensional standard diffusion equation for the concentration of inhibitor,

$$\frac{dZ(x,t)}{dt} = \frac{d}{dx}\left[D_z \frac{dZ(x,t)}{dx} \right] - k_{z,D} D^*(x,t) Z(x,t) - k_{z,R^\bullet} Z(x,t) R^\bullet(x,t) - k_{z,M^\bullet} Z(x,t) M^\bullet(x,t), \tag{13}$$

where Z is the instantaneous inhibiting oxygen concentration and D_z is the diffusion constant of oxygen in the dry material layer, which in this analysis will be assumed to be time and space independent. This assumption is reasonable, as this fast rate of diffusion of the small oxygen molecule will not be significantly affected by any small changes in material viscosity. The inhibition rate constants, $k_{z,R^\bullet}$ and $k_{z,M^\bullet}$, will in general have different values (of reactivity) due to the differences in the relative molecular size, [37]. However in this analysis, for the sake of simplicity we

assume $k_z = k_{z,R^\bullet} = k_{z,M^\bullet}$. Furthermore it is expected that the reactivity of oxygen with the excited state form of the photosensitiser will be much lower, i.e. $k_{z,D} << k_z$ and therefore we assume it is negligible.

2.2.3 Primary Radicals

The equation governing the concentration of primary radicals can be given by,

$$\frac{dR^\bullet(x,t)}{dt} = k_d D^*(x,t) CI(x,t) - k_{iA} R^\bullet(x,t) u_A(x,t) - k_{iB} R^\bullet(x,t) u_B(x,t) - k_{tp} R^\bullet(x,t) M^\bullet(x,t) - k_z R^\bullet(x,t) Z(x,t), \quad (14)$$

where $u_A(x, t)$ and $u_B(x, t)$ are the monomer and crosslinker concentrations, (denoted earlier in the chemical reactions by M_A and M_B respectively). This equation states that the rate of change of primary radical concentration is proportional to the concentration of primary radicals generated by photon absorption, minus the amounts removed by: the initiation of macroradicals, by primary termination with growing polymer chains, and by inhibiting oxygen.

2.2.4 Macroradicals

With the inclusion of both types of termination mechanism (primary and bimolecular) and the effects of oxygen inhibition, the equation governing macroradical concentration is given by,

$$\frac{dM^\bullet(x,t)}{dt} = k_{iA} R^\bullet(x,t) u_A(x,t) + k_{iB} R^\bullet(x,t) u_B(x,t) - 2k_t \left[M^\bullet(x,t)\right]^2 - k_{tp} R^\bullet(x,t) M^\bullet(x,t) - k_z Z(x,t) M^\bullet(x,t) \quad (15)$$

where again $u_A(x, t)$ and $u_B(x, t)$ denotes the monomer and crosslinker concentrations and the squared term on the right hand side represents the effects of bimolecular termination. The generation terms in this equation previously appear as the removal terms due to macroradical initiation in Eq (14).

2.2.5 Monomer, Crosslinker and Holes

The effect of material shrinkage is a physical characteristic of the free radical polymerization process [3,35]. As briefly mentioned earlier, the covalent single carbon bond linking the molecules in a polymer chain can be up to 50% shorter than the van der Waals bond which exists between the monomer and crosslinker molecules in an unpolymerised state [36]. Thus, as polymerization takes place the overall density of the material increases rapidly (which causes a modulation in refractive index), and the material's volume decreases causing shrinkage in the areas polymerised. This shrinkage effect can lead to Bragg detuning between grating recording and replay particularly when recording unslanted or reflection type gratings and is therefore of crucial importance when attempting to model the behaviour of these photopolymers.

Recently, much work has been carried out to account for the effects of shrinkage during and post holographic exposure in photopolymers [36-38]. Qi *et al*. [38] modelled the processes of material shrinkage using the concept of holes. They suggested that free volume is created in the form of temporary holes, which then collapse instantaneously resulting in an overall reduction in the systems volume. Sutherland *et al*. [36] extended this concept to account for the fact that shrinkage does not necessarily occur instantaneously by allowing for the collapse of the holes at some characteristic rate constant, depending on the material. Karpov *et al*. [37] had, previous to this, also used the hole concept to model the shrinkage process. However unlike the previous authors, Karpov *et al*. developed a two component PDD model which allowed for hole diffusion prior to their collapse. Following on from this analysis, Kelly *et al*. [28] examined two methods to account for the shrinkage behaviour. The first assumed that hole collapse occurs quickly as the vacuum is filled and therefore the diffusion of holes is negligible. The second, included the effects of hole diffusion after they were create. The predictions produced by both models were then examined and contrasted.

In this analysis, we assume that as the monomer and crosslinker are polymerised the associated volume changes are accounted for by the creation of free space holes. In this way, the total volume of the material is conserved throughout, yielding the expression,

$$\phi_{mA}(t)+\phi_{mB}(t)+\phi_{p}(t)+\phi_{b}+\phi_{HoleA}(t)+\phi_{HoleB}(t)=1,$$

(16)

where ϕ_{mA}, ϕ_{mB}, ϕ_{p}, ϕ_{b}, ϕ_{HoleA} and ϕ_{HoleB} are the respective volume fractions of monomer, crosslinker, polymer, background, holes created by the polymerisation of monomer and crosslinker. These volume fractions are determined using the expression, $\phi_i = x_i v_i \Big/ \sum_i x_i v_i$, where x_i is the mole fraction and v_i is the molar volume of the i^{th} component. The material is therefore modelled as being made up of monomer, crosslinker, polymer, holes and an unchanging background material. Also, it must be noted that the polymer volume fraction, $\phi_{\mathrm{p}}(t)$, consists of the contributions of polymerised monomer, $\phi_{\mathrm{pA}}(t)$, and polymerised crosslinker, $\phi_{\mathrm{pB}}(t)$, as discussed earlier in Section 2.1, i.e., $\phi_{\mathrm{p}}(t) = \phi_{\mathrm{pA}}(t) + \phi_{\mathrm{pB}}(t)$.

Furthermore, it is assumed that the volume fraction of monomer with time, $\phi_{\mathrm{mA}}(t)$, is converted directly into the volume fraction of polymerised monomer, $\phi_{\mathrm{pA}}(t)$, and holes, $\phi_{\mathrm{HoleA}}(t)$, yielding the expression,

$$\phi_{mA}(t)=\phi_{pA}(t)+\phi_{HoleA}(t),$$

(17)

and the volume fraction of crosslinker, $\phi_{\mathrm{mB}}(t)$, is converted directly into the volume fraction of polymerised crosslinker, $\phi_{\mathrm{pB}}(t)$, and holes, $\phi_{\mathrm{HoleB}}(t)$,

$$\phi_{mB}(t)=\phi_{pB}(t)+\phi_{HoleB}(t).$$

(18)

Following on from the work presented by Karpov *et al*. [37] on multicomponent diffusion, it is then assumed that the diffusion of monomer and crosslinker into the bright regions of the interference pattern (in an attempt to equalising the concentration gradients), must be met with a counter flow of $Hole_A$ and $Hole_B$, which is equal and opposite. Thus the total net flux in the material is zero and the condition of total volume conservation is satisfied.

We therefore construct a set of mutual diffusion equations, whereby the flow density of each component will be dependent on the concentrations of each of the other components and their gradients. Assuming that the flow of monomer, j_{uA} is coupled to the flow of $Hole_{\mathrm{A}}$, j_{HoleA}, with a mutual diffusion coefficient D_{mA}, we obtain,

$$j_{uA}=-j_{HoleA}=-D_{mA}\left[Hole_A(x,t)\nabla u_A(x,t)-u_A(x,t)\nabla Hole_A(x,t)\right],$$

(19)

where $u_{\mathrm{A}}(x,t)$ and $Hole_{\mathrm{A}}(x,t)$ are the concentrations of monomer and *HolesA* respectively. The equivalent expression for mutual diffusion of the crosslinker, $u_{\mathrm{B}}(x,t)$, and $Hole_B(x,t)$ concentrations can be given as,

$$j_{uB}=-j_{HoleB}=-D_{mB}\left[Hole_B(x,t)\nabla u_B(x,t)-u_B(x,t)\nabla Hole_B(x,t)\right],$$

(20)

where D_{mB} is the mutual diffusion coefficient associated with the flow of crosslinker, j_{uB}, and $Hole_B$, j_{HoleB}. Note that as the crosslinker is much less mobile than the monomer, we expect that $D_{\mathrm{mB}} < D_{\mathrm{mA}}$. If diffusion of holes is neglected, we see that Eqs (19) and (20) will return to a Fick's law based relation. In order to include the effects of viscosity on the diffusion coefficients D_{mA} and D_{mB}, a Doolittle-type equations is used to cast these diffusion coefficients in terms of the fractional free volume, *f*, which is presented in Eq (5), [39,40]. Thus yielding,

$$D_{mA}=D_{mA0}\exp\left[-A_{DmA}/f\right],$$

(21a)

and

$$D_{mB}=D_{mB0}\exp\left[-A_{DmB}/f\right],$$

(21b)

where, D_{mA0} and D_{mB0} are the pre-exponential factors for the diffusion of monomer and crosslinker respectively, and A_{DmA} and A_{DmB} are parameters which govern the rate of decrease of the diffusion of monomer and crosslinker with decreasing free volume.

With the inclusion of the above, we can now construct the 1D diffusion equations for the monomer, crosslinker, holes and polymer. The coupled differential equation representing the monomer concentration, $u_{\mathrm{A}}(x,t)$ can be given by,

$$\frac{du_A(x,t)}{dt} = \nabla j_{uA}(x,t) - k_{iA}R^{\bullet}(x,t)u_A(x,t) - \int_{-\infty}^{\infty} k_{pA}M^{\bullet}(x',t)u_A(x',t)G(x,x')dx',$$

(22)

where $\nabla j_{uA}(x,t)$ is the divergence of monomer and $G(x,x')$ is the non-local material spatial response function given by:

$$G(x,x') = \frac{1}{\sqrt{2\pi\sigma}}\exp\left[\frac{-(x-x')^2}{2\sigma}\right],$$

(23)

with σ as the constant non-local response parameter which is normalized with respect to the grating period, Λ. As before [26], the non-local spatial response function represents the effect of initiation at location x' on the amount of monomer polymerized at location x.

The coupled differential equation representing the crosslinker concentration, $u_B(x,t)$ can be given by,

$$\frac{du_B(x,t)}{dt} = \nabla j_{uB}(x,t) - k_{iB}R^{\bullet}(x,t)u_B(x,t) - \int_{-\infty}^{\infty} k_{pB}M^{\bullet}(x',t)u_B(x',t)G(x,x')dx',$$

(24)

where $\nabla j_{uB}(x,t)$ is the divergence of monomer.

The corresponding coupled differential equations for the free space holes created by polymerisation of the monomer and crosslinker, i.e. $Hole_A(x,t)$ and $Hole_B(x,t)$ respectively, can then be given as,

$$\frac{dHole_A(x,t)}{dt} = \nabla j_{HoleA}(x,t) + k_{iA}R^{\bullet}(x,t)u_A(x,t) + k_{pA}M^{\bullet}(x,t)u_A(x,t),$$

(25)

and

$$\frac{dHole_B(x,t)}{dt} = \nabla j_{HoleB}(x,t) + k_{iB}R^{\bullet}(x,t)u_B(x,t) + k_{pB}M^{\bullet}(x,t)u_B(x,t),$$

(26)

where $\nabla j_{HoleA}(x,t)$ is the divergence of monomer and $\nabla j_{HoleB}(x,t)$ is the divergence of the crosslinker.
The equation governing the polymer concentration can then be given by,

$$\frac{dN(x,t)}{dt} = \frac{d}{dx}\left[D_N\frac{dN(x,t)}{dx}\right] + \int_{-\infty}^{\infty} k_{pA}M^{\bullet}(x',t)u_A(x',t)G(x,x')dx' + \int_{-\infty}^{\infty} k_{pB}M^{\bullet}(x',t)u_B(x',t)G(x,x')dx',$$

(27)

where the polymer diffusion coefficient, D_N, is again represented in a Doolittle type equation [39,40] to account for the reduction in fractional free volume, f, as a result of polymerisation, where,

$$D_N = D_{N0}\exp[-A_{DN}/f],$$

(28)

where A_{DN} represents the rate of decrease of the polymer diffusion with decreasing free volume, and D_{N0} is the pre-exponential factor. We note that the mobility of the polymer chains in the presence of an appropriate concentration of crosslinker is expected to be negligible, which will result in the production of stable holographic gratings, therefore $D_N << D_{mB} < D_{mA}$.

Since the above coupled differential equations presented in Eqs (9-15), (22) and (24-27), depend upon the spatial distribution of the exposing intensity, they will all be periodic even functions of x and can therefore be written as Fourier series, i.e., $X(x,t) = \sum_{j=0}^{\infty} X_j(t)\cos(jKx)$, where X represents the species concentrations, D, D^*, CI, $HD^{\bullet}$,

$R^{\bullet}$, $M^{\bullet}$, u_A, u_A, $Hole_A$, $Hole_B$, N and Z. A set of first-order coupled differential equations can then be obtained in the same manner presented in Refs [9-11], by gathering the coefficients of the various co-sinusoidal spatial contributions and writing the equations in terms of these time varying spatial harmonic amplitudes. These coupled equations can then be solved using the following initial conditions,

$$Z_0(t=0)=Z_0,\ D_0(t=0)=D_0,\ CI_0(t=0)=CI_0,\ u_{A0}(t=0)=U_{A0},\ u_{B0}(t=0)=U_{B0},$$
$$D_{n>0}(t=0)=D^{*}_{n\geq 0}(t=0)=HD^{\bullet}_{n\geq 0}(t=0)=CI_{n>0}(t=0)=0, \text{ and}$$
$$Z_{n>0}(t=0)=R^{\bullet}_{n\geq 0}(t=0)=M^{\bullet}_{n\geq 0}(t=0)=Hole_{An\geq 0}(t=0)=Hole_{Bn\geq 0}(t=0)=N_{n\geq 0}(t=0)=0. \quad (29)$$

As in previous analysis, the Fourier series expansion of the monomer and polymer harmonics involve the use of the non-local response parameter $G(x,x')$ which is represented in the coupled differential equations by $S_i=\exp\left(-i^2K^2\sigma/2\right)$.

In the next section we examine some predictions generated as a result of the developments made to the NPDD model.

3. MODEL PREDICTIONS AND CONCLUSIONS

Utilising the developed NPDD derived in the previous section, we now look at some of the key new predictions that the model can produce, indicating the increased physicality of the model. The first of these is shown in Figure 1, whereby the time evolution of the first two normalised spatial concentration harmonics of the monomer, u_A and crosslinker, u_B are presented. The exposure intensity used is I_0 = 1 mW/cm^2 at a spatial frequency, SF = 1428 lines/mm, with fringe visibility, V = 1 in an acrylamide based photopolymer material such as those examined in Refs [9-11].

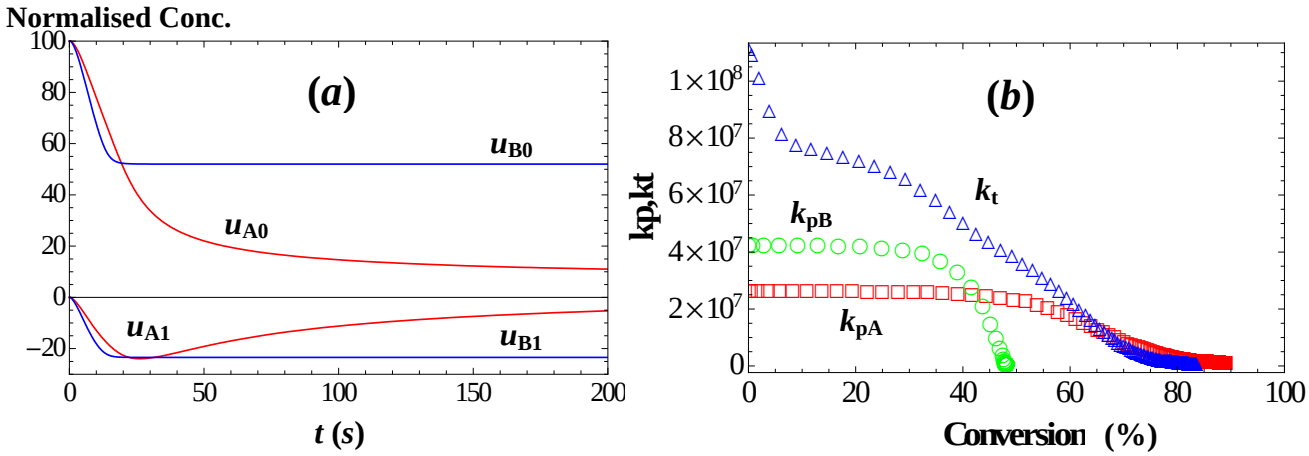

Figure 1(a). Simulation of the first two spatial concentration harmonics of monomer, u_A (red curve) and crosslinker, u_B (blue curve). Figure 1(b) shows the temporal variation of propagation and termination rates against monomer and crosslinker conversion. Red squares represent, k_{pA}, Green circles represent, k_{pB}, Blue triangles represent, k_t, (scaled down by a factor of 50 for illustration).

As can be observed in Figure 1(a), as the exposure time, t (s) is increased, the normalised monomer and crosslinker concentrations, u_A and u_B, decrease, due to photo-polymerisation. As discussed in Section2, this polymerisation causes an increase in the material's viscosity, which acts to decrease the rate at which polymerisation proceeds. This decrease occurs due to the reduction in the kinetic rates of initiation, propagation and termination, and the fall off in diffusional effects with the reduced fractional free volume. Examined Figure 1(b), we see the effect of viscosity on the kinetic rates, k_{pA}, k_{pB} and k_t. Analysing the propagation rate of the monomer, k_{pA}, we see that as the conversion of carbon double bonds (monomer to polymer) reaches ~ 40% a dramatic reduction in its rate can be observed. This is the point at which diffusional limitations set in. The same effect occurs for k_{pB} but at an earlier conversion due to the complex structure of the crosslinker and its low mobility. Analysing k_t we see that its evolution is not as simplistic. There is an initial drop off which is caused by growing polymer chains experiencing diffusional limitations and autoacceleration

occurs. Then the effect of reaction-diffusion termination starts to dominate and the initial rapid decrease is curtailed. Examining Eq (4), we see that this corresponds to proportionality between the reaction-diffusion termination and the unreacted monomer and crosslinker concentrations, which decrease as the exposure continues. Then as the propagation rates, k_{pA} and k_{pB}, start to decrease in the autodeceleration region, k_t starts to decrease in proportion with the reaction-diffusion. The effects of the variations in the kinetic rates presented in Figure 1(b) can be easily observed in Figure 1(a), inclusive of the rapid removal of monomer and crosslinker leading to autoacceleration, followed diffusional limitations leading to autodeceleration. Taking a brief look at the first harmonics of the monomer and crosslinker in Figure 1(a), we note the presence of diffusion effects which act to equalise the concentration gradients set up by polymerisation. It can be clearly seen that the viscosity effects have caused a reduction in the mobility of monomer molecules, and more significantly a severe reduction to the movement of the larger crosslinker molecules.

A lot of work still remains to be done, including a full examination of the predictions of this NPDD model. In particular; a) a full analysis of the effects of viscosity on the refractive index modulation, b) the effects of the introduction of free space holes, and c) an examination of the effects of operating temperatures and various concentration ratios to optimise material performance.

Acknowledgments

The authors acknowledge the support of the Irish Research Council for Science, Engineering and Technology through the Empower Postdoctoral research scholarship. We also acknowledge the support of Enterprise Ireland and Science Foundation Ireland through the national development plan.

References

[1] C. H. Bamford, A. D. Jenkins, R. Johnston, "Termination by primary radicals in vinyl polymerization," Trans. Faraday Soc. **55**(8), 1451-1460, (1959).

[2] C. Decker, B. Elzaouk and D. Decker, "Kinetic study of ultrafast photopolymerizations reactions," Journal of Macromolecular Science, Pure and Applied Chemistry **A33**(2), 173-190, (1996).

[3] M. D. Goodner, H. R. Lee, C. N. Bowman, "Method for determining the kinetic parameters in diffusion-controlled free-radical homopolymerizations," Industrial and Engineering Chemistry Research **36**(4), 1247-1252, (1997).

[4] M. D. Goodner and C. N. Bowman, "Modeling primary radical termination and its effects on autoacceleration in photopolymerization kinetics," Macromolecules **32**(20), 6552-6559, (1999).

[5] J. R. Lawrence, F. T. O'Neill, J. T. Sheridan, "Photopolymer holographic recording material," Optik **112**(10), 449-463, (2001).

[6] S. Blaya, L. Carretero, R. F. Madrigal, M. Ulibarrena, P. Acebal, A. Fimia, "Photopolymerization model for holographic gratings formation in photopolymers," Appl. Phys. B-Lasers and Optics **77**(6-7), 639-662, (2003).

[7] M. R. Gleeson, J. V. Kelly, D. Sabol, C. E. Close, S. Liu, J. T. Sheridan, "Modelling the photochemical effects present during holographic grating formation in photopolymer materials," J. Appl. Phys. **102**(2), 023108, (2007).

[8] M. R. Gleeson, D. Sabol, S. Liu, C. E. Close, J. V. Kelly, J. T. Sheridan, "Improvement of the spatial frequency response of photopolymer materials by modifying polymer chain length," J. Opt. Soc. Am. **B 25**(3), 396-406, (2008).

[9] M. R. Gleeson, and J. T. Sheridan, "Non-local photo-polymerization kinetics including multiple termination mechanisms and dark reactions: Part I. Modelling," J. Opt. Soc. Am. **B26**(9), 1736-1745, (2009).

[10] M. R. Gleeson, S. Liu, R. R. McLeod, J. T. Sheridan, "Non-local photo-polymerization kinetics including multiple termination mechanisms and dark reactions: Part II. Experimental Validation," J. Opt. Soc. Am. **B26**(9), 1746-1754, (2009).

[11] M. R. Gleeson, S. Liu, J. Guo, and J. T. Sheridan, "Non-local photo-polymerization kinetics including multiple termination mechanisms and dark reactions: Part III. Primary radical generation and inhibition," J. Opt. Soc. Am. **B** 27(9), 1804-1812, (2010).

[12] L. Dhar, A. Hale, H. E. Katz, M. L. Schilling, M. G. Schnoes, and F. C. Schilling, "Recording media that exhibit high dynamic range for digital holographic data storage," Optics Letters **24**(7), 487-489, (1999).

[13] S. Schultz, E. Glytsis, T. Gaylord, "Design, fabrication, and performance of preferential-order volume grating waveguide couplers," Applied Optics **39**, 1223-1232, (2000).

[14] A. Sato, M. Scepanovic, R. Kostuk, "Holographic edge-illuminated polymer bragg gratings for dense wavelength division optical filters at 1550 nm," Applied Optics **42**, 778-784 (2003).

[15] R. R. McLeod, A. J. Daiber, M. E. McDonald, T. L. Robertson, T. Slagle, S. L. Sochava, L. Hesselink, "Microholographic multilayer optical disk data storage," Applied Optics **44**, 3197-3207, (2005).
[16] F. Bruder and T. Faecke, "Materials in Optical Data Storage," Int. J. Mat. Res., **101**(2), (2010).
[17] InPhase Technologies, "www.inphase-technologies.com" Tapestry Media, (2007).
[18] M. Gu, M. Straub, L. H. Nguyen, "Complex-shaped 3-D microstructures and photonic crystals generated in a polysiloxane polymer by two-photon microstereolithography," Opt. Materials, **27**, 359-364, (2004).
[19] J. Zhang, K. Kasala, A. Rewari, K. Saravanamuttu, "Self-trapping of spatially and temporally incoherent white light in a photochemical medium," J. Am. Chem. Soc. **128**(2), 406-407, (2006).
[20] G. H. Zhao and P. Mouroulis, "Diffusion-model of hologram formation in dry photopolymer materials," Journal of Modern Optics **41**(10), 1929-1939, (1994).
[21] S. Piazzolla and B. K. Jenkins, "Holographic grating formation in photopolymers," Optics Letters **21**(14), 1075-1077, (1996).
[22] V. L. Colvin, R. G. Larson, A. L. Harris, and M. L. Schilling, "Quantitative model of volume hologram formation in photopolymers," Journal of Applied Physics **81**(9), 5913-5923, (1997).
[23] D. J. Lougnot, P. Jost, and L. Lavielle, "Polymers for holographic recording. VI. Some basic ideas for modelling the kinetics of the recording process," Pure and Applied Optics **6**(2), 225-245, (1997).
[24] I. Aubrecht, M. Miler, I. Koudela, "Recording of holographic diffraction gratings in photopolymers: Theoretical modelling and real-time monitoring of grating growth," Journal of Modern Optics **45**(7), 1465-1477, (1998).
[25] J. H. Kwon, H. C. Hwang, and K. C. Woo, "Analysis of temporal behaviour of beams diffracted by volume gratings formed in photopolymers," Journal of the Optical Society of America **B 16**(10), 1651-1657, (1999).
[26] J. T. Sheridan and J. R. Lawrence, "Nonlocal response diffusion model of holographic recording in photopolymer," Journal of the Optical Society of America **A 17**(6), 1108-1114, (2000).
[27] C. Neipp, S. Gallego, M. Ortuno, A. Marquez, M. L. Alvarez, A. Belendez, and I. Pascual, "First-harmonic diffusion-based model applied to a polyvinyl-alcohol - acrylamide-based photopolymer," Journal of the Optical Society of America **B 20**(10), 2052-2060, (2003).
[28] J. V. Kelly, M. R. Gleeson, C. E. Close, F. T. O'Neill, J. T. Sheridan, S. Gallego, and C. Neipp, "Temporal analysis of grating formation in photopolymer using the nonlocal polymerization-driven diffusion model," Optics Express **13**(18), 6990-7004, (2005).
[29] J. T. Sheridan, M. R. Gleeson, C. E. Close, J. V. Kelly, "Optical response of photopolymer materials for holographic data storage applications," Journal of Nanoscience and Nanotechnology **7**(1), 232-242, (2007).
[30] M. R. Gleeson and J. T. Sheridan, "A review of the modelling of free-radical photo-polymerisation in the formation of holographic gratings," J. Opt. A **10**, 024008, (2009).
[31] J. Guo, M. R. Gleeson, S. Liu and J. T. Sheridan, "Non-Local Spatial Frequency Response of Photopolymer materials containing Chain Transfer Agents: Part I. Theoretical Model," J. Opt. A: Pure Appl. Opt., **13**(9), 095601, (2011).
[32] J. Guo, M. R. Gleeson, S. Liu and J. T. Sheridan, "Non-Local Spatial Frequency Response of Photopolymer materials containing Chain Transfer Agents: Part II. Experimental Results," J. Opt. A: Pure Appl. Opt., **13**(9), 095602, (2011).
[33] M. R. Gleeson, J. Guo and J. T. Sheridan, "Optimisation of Photopolymers for Holographic Applications using the Non-Local Photo-Polymerization Driven Diffusion Model," Opt. Exp. **19**(23), 22423-22436, (2011).
[34] M. R. Gleeson, J. T. Sheridan, F. Bruder, T. Roelle, D. Honnell, M. S. Weiser, T. Faecke, "Comparison of a new self-developing photopolymer with AA/PVA based photopolymer utilizing the NPDD model," Opt. Exp. **19**(27), 26325-26342, (2011).
[35] G. Odian, *Principles of Polymerization*, Wiley, New York, (1991).
[36] R. L. Sutherland, V. P. Tondiglia, L. V. Natarajan, T. J. Bunning, "Phenomenological model of anisotropic volume hologram formation in liquid-crystal-photopolymer mixtures," J. Appl. Phys. **96**(2), 951-965, (2004).
[37] G. M. Karpov, V. V. Obukhovsky, T. N. Smirnova, and V. V. Lemeshko, "Photoformers-materials for holographic recording," Proc. SPIE **2795**, 294-305, (1996).
[38] J. Qi, L. K. Li, M. De Sarkar, and G. P. Crawford, "Nonlocal photopolymerization effect in the formation of reflective holographic polymer-dispersed liquid crystals," Journal of Applied Physics **96**(5), 2443-2450, (2004).
[39] F. Bueche, "Physical properties of polymers," New York: Interscience, 354, (1962).
[40] M. D. Goodner and C. N. Bowman, "Development of a comprehensive free radical photopolymerization model incorporating heat and mass transport effects in thick films," Chem. Eng. Sci. **57**(5), 887-900, (2002).